FUDMA Journal of Sciences (FJS)
ISSN online: 2616-1370
ISSN print: 2645 - 2944
Vol. 9 No. 12, December (Special Issue), 2025, pp 621 – 628
DOI: https://doi.org/10.33003/fjs-2025-0912-4318

COMPARISON OF PARTICULATE MATTER ($PM_{2.5}$) GROUND DATA AND SATELLITE DATA IN KANO STATE, NIGERIA

***[1]Maryam Idris, [2]Muawiya Sani and [3]Rakiya Aliyu**

[1]Department of Physics, Bayero University, Kano, PMB 3011 Kano State-Nigeria
[2]Centre for Atmospheric Research, National Space Research and Development Agency, Kogi State University, Anyigba, Kogi State, Nigeria.
[3]Department of Physics, Kano University of Science and Technology Wudil.

*Corresponding authors' email: midris.phy@buk.edu.ng

ABSTRACT

Air pollution, particularly fine particulate matter ($PM_{2.5}$), poses significant environmental and health risks. This study compares satellite-derived $PM_{2.5}$ data with ground-based measurements at different heights (2m, 5m, and 10m) to evaluate their accuracy and seasonal variations. Results indicate that during the dry season (Harmattan), $PM_{2.5}$ concentrations reached 270 µg/m³, 117.11µg/m³ and 90µg/m³ highlighting increased pollution due to dust transport and atmospheric stability. In contrast, during the rainy season, $PM_{2.5}$ levels dropped significantly to 6.59µg/m³, 12.5µg/m³, 14.2µg/m³ and 15.42µg/m³ demonstrating the effect of wet deposition. The study underscores the importance of integrating satellite and ground-based $PM_{2.5}$ data for accurate air quality assessments and policy-making. It delves into the effects of particulate matter, sources of particulate matter on satellite data and elucidates meteorology and meteorological parameters used for describing and quantifying atmospheric conditions.

Keywords: Ground-based measurements, Harmattan (dry season), Meteorological parameters particulate matter, Satellite-derived data.

INTRODUCTION

The impact of air pollutants in the ambient air is of high concern due to their adverse effect on human health and the environment. Air pollutants are hazardous substances in the air that are produced from natural sources such as radon gas or from anthropogenic sources (man-made) such as combustion for energy production in industry, internal combustion engines and standby generators (Idris *et al.,* 2022).

Pollution is the release of harmful or toxic substances into the environment, which leads to adverse effects on ecosystems, human health, and natural resources. These harmful substances, known as pollutants, can originate from various sources and come in different forms, such as chemicals, particles, noise, or energy. Pollution occurs when these contaminants exceed the environment's natural capacity to absorb and neutralize them, thereby causing harm or imbalances (Idris, *et al.,* 2020).

Particulate matter (PM) refers to tiny particles or droplets in the air that vary in size and composition. These particles are usually a mix of dust, dirt, soot, smoke, and liquid droplets.

Particulate matter or particle pollution are mixture of microscopic solid and liquid particles present in air. The presence of PM in air can be monitored through modern devices known as air quality sensors (Lawal *et al.,* 2023). Particulate matter can originate from various sources, including vehicle exhaust, industrial emissions, construction activities, and natural processes like wildfires or volcanic eruptions. It is typically classified into two types, particulate matter 2.5 and particulate matter 10.

In today's industrialized and heavily populated world, pollution is one of the most significant environmental challenges. The rapid growth of industries, transportation, urbanization, and agricultural practices has accelerated the release of pollutants into air, water, and soil. These pollutants not only degrade the quality of life but also threaten biodiversity, contribute to climate change, and cause long-term ecological damage.

This study examined the relationship between ground-based and satellite-derived $PM_{2.5}$ data at different heights (2m, 5m, and 10m) to evaluate their accuracy and seasonal variations in Kano State, Nigeria, over a 12-month period from July 2021 to July 2022. The research also identified notable seasonal patterns, showing significantly higher $PM_{2.5}$ concentrations during the Harmattan season.

Literature Review

Cohen *et al.,* (2017) carried out an experiment which estimated that exposure to outdoor air pollution is responsible for about 4 million premature deaths annually with about another 3-4 million resulting from exposure to indoor air pollution; that is, air pollution is responsible for about 1 in 9 deaths worldwide. The majority of deaths are associated with fine particulate matter of less than 2.5 µm in width ($PM_{2.5}$). Knowledge of both $PM_{2.5}$ concentrations and the concentrations of a number of pollutants is required to devise effective mitigation strategies for $PM_{2.5}$ since it is directly emitted to the atmosphere, such as in the form of smoke and dust, which also form in the atmosphere through chemical reactions that transform gaseous pollutants (e.g., sulfur dioxide (SO_2), ammonia (NH_3), nitrogen dioxide (NO_2)) to particles (i.e., gas to particle conversion).

Zang *et al.,* (2021) investigated how the adverse effects from exposure to particulate matter 2.5 µm in diameter ($PM_{2.5}$) on health-related outcomes have been found in a range of experimental and epidemiological studies. It was aimed at assessing the significance, validity, and reliability of the relationship between long-term $PM_{2.5}$ exposure and various health outcomes.

Hongye Zhou *et al.,* (2022) investigated how the background of $PM_{2.5}$ concentration represents the combined emissions from natural domestic and foreign sources, which has implications for the maximum effect, in terms of air-quality control, that can be achieved by reducing emissions. However, estimating the background $PM_{2.5}$ concentrations via background monitoring sites for a densely populated

region (e.g., Taiwan) has been a challenge. In this study, we compared two statistical methods of estimating the background concentration using an 11-year time series (2005–2016) of data from three air-quality stations in Taiwan. Sheng-Hsiang Wang *et al.,* (2020) carried out a study that plays a crucial role in the understanding that air quality model solves the mathematical equations of chemical and physical processes in pollution transportation numerically. While the data-driven model, as another scientific research paradigm with powerful extraction of complex high-level abstractions, has shown unique advantages in the $PM_{2.5}$ prediction applications. In this paper, to combine the two advantages of strong interpretability and feature extraction capability.

Theoretical Background

Tropospheric aerosols can be characterized through ground-based and satellite-based measurements. This involves the use of interpretation and inversions of electromagnetic radiance measurements by which the radiation is characterized at specific wavelength that is sensitive to the object of interest. Thus, the method requires the use of radiative transfer theory and the fundamentals of light scattering.

Most radiation utilize for aerosol retrieval methodology is either emitted by the sun or objects in the earth's atmosphere or on/near earth's surface and this is generally affected either scattering or absorption.

$$\beta_\lambda(T) = \frac{2hc^2}{\lambda^5}\frac{1}{e^{hc/\lambda kT}-1} \quad (1)$$

Equation (1) is Plank's law in terms of wavelength (λ) given as the intensity of radiation per unit area per unit wavelength from a black body at a temperature(T), where the k is Boltzmann constant, *h* is Plank's constant, and c is the speed of light with values 1.38 x 10^{-23} $m^2kg^{-2}k^{-1}$, 6.626 x 10^{-34} m^2 kgs^{-1} and 3 x 108 ms^{-1} respectively.

From radiative transfer theory of a black body is a perfect absorber and a perfect emitter obeying Kirchhoff's law equation (2) which states emissivity (ε_λ) of an object is exactly equal to its absorptivity(α_λ) .

$$L_{i\lambda} = L_{r\lambda} + L_{\alpha\lambda} + L_{T\lambda} \quad (2)$$

where is $L_{i\lambda}$ is the incident radiant flux at a specific wavelength (λ), $r\lambda$ is the spectral hemispherical reflectance, $\alpha\lambda$ is the spectral hemispherical absorptance and $T\lambda$ is the spectral hemispherical transmittance.

The wavelength of maximum emission (λ_m) can be described by Wein's law equation (3) as constant divided by black body's temperature (T).

$$\lambda_m T = 2897.9\ \mu mK \quad (3)$$

The theory of Rayleigh scattering suggested that the scattering of electromagnetic radiation such as solar energy by air molecules or particles in the air varies with wavelengths equation (4) (Musa, 2010) .

$$\sigma^a(\lambda) = C/\lambda^4 \quad (4)$$

where C is a parameter depending on wavelengths (λ)

The radiance observe at the satellite is whatever comes from the surface plus the sources along the path to the satellite caused by absorption and scattering minus the sinks caused by absorption and scattering. The change in radiance (dL) will be the radiance at the top of the atmosphere (L_{top})where the satellite is minus the radiance in the atmosphere (L)equation (5).

$$dL = L_{top} - L \quad (5)$$

Since we are interested in the change in radiance in the atmosphere (dL) at a point X, the change in radiance is the function of location and a direction along the path towards the satellite (r) as described by Schwarzchild's equation (6).

$$dL(X,r) = -\sigma_{e,\lambda}(X)L_\lambda(X,r) + J_\lambda(X,r) \quad (6)$$

where $L_\lambda(X,r)$ is the initial radiance at point X in the direction r and $J_\lambda(X,r)$ is the total source radiance at point X in the direction r and $\sigma_{e,\lambda}(X)$ is the volume extinction at the point X usually referred as beam attenuation coefficient given by equation (7).

$$\sigma_{e,\lambda}(X) = \sigma_{a,\lambda} + \sigma_{s,\lambda} \quad (7)$$

where $\sigma_{a,\lambda}$ is the volume absorption coefficient and $\sigma_{s,\lambda}$ is the volume scattering coefficient.

The probability of interaction between the radiance photon and the aerosol's particle been a scattering interaction is given by Single Scattering Albedo (ω_0) which is the ratio of scattering efficiency ($\sigma_{s,\lambda}$) to total extinction efficiency($\sigma_{e,\lambda}$) equation (8).

$$\omega_0 = \frac{\sigma_{s,\lambda}(X)}{\sigma_{e,\lambda}(X)} \quad (8)$$

For sources of radiation $J_\lambda(X,r)$ in equation (6):

$$J_\lambda(X,r) = J_{th}(X,r) + J_{scat}(X,r) \quad (9)$$

where $J_{th}(X,r)$ is the sources from thermal and $J_{scat}(X,r)$ sources from scattering and the thermal source is given by equations (10) and (11).

$$J_{th}(X,r) = \sigma_{a,\lambda}\ B_\lambda(T(X)) \quad (10)$$

$$J_{scat}(X,r) = \int_{4\pi}\gamma_{s,\lambda}\,(r,r',X)L_\lambda(r'X)d\Omega' \quad (11)$$

Recall from Kirchhoff's law $\sigma_{a,\lambda}$ at a given temperature we have equation (12).

$$\left|\sigma_{a,\lambda}\right| = \varepsilon_\lambda \quad (12)$$

Optical Depth

Optical depth is the unit less quantity showing how much absorption and scattering of radiation occurs at some specified wavelength along the path mathematically given as equation (13) (Lazrak *et al.,* 2019).

$$\delta_\lambda(z) = \int_z^\infty \sigma_{e,\lambda}(z')dz' \quad (13)$$

where z is 0, and the integral is from 0 to for optical depth of the atmosphere. Hence, Atmospheric aerosol optical depth tells us how much direct sunlight is prevented from reaching the ground by these aerosol particles Liu *et al.,* (2005):

Direct Transmittance also called transmissivity is given by equation (14).

$$T_d = e^{\delta_\lambda(z')/\mu} \quad (14)$$

where $\mu = cos\theta$, and θ is the slant path angle of radiation. Then finally, the path optical depth is given as:

$$\delta_s(s) = \int_{s_1}^{s_2}\sigma_{e,\lambda}(s')ds' \quad (15)$$

where s' is the coordinate along the path maybe larger than the optical depth of the atmosphere, hence, the direct transmittance along the path will be lower.

As such,

$$\delta_s(s) = \int_{s_1}^{s_2}\sigma_{e,\lambda}(s')ds' = \frac{1}{\mu}\int_0^\infty \sigma_{e,\lambda}(z')dz' \quad (16)$$

Assuming no sources of radiation happen along the path, then equation (5) becomes equation (17).

$$dL(s,r) = -\sigma_{e,\lambda}(s)L_\lambda(s,r) \quad (17)$$

And this gives Beer's law equation (18) that states that the radiance at the end of the path is the radiance at the beginning of the path multiplied by the direct transmittance.

$$L(s_1) = L(s)e^{\delta(s)} \quad (18)$$

where $L(s)$ is the initial radiance, $L(s_1)$ is the final radiance and $e^{\delta(s)}$ is the direct transmittance from point s to the boundary s_1 respectively.

Experimentally, the voltage (V) measured by a sun photometer is proportional to the spectral irradiance reaching the instrument at the surface. The estimated top of the atmosphere spectral irradiance in terms of voltage (V_o) is obtained by sun photometer measurements such that the total optical depth (τ_{total}) can be obtained using equation (19) according to equation (18) as:

$V(\lambda) = V_O d^2 \exp\left[-\tau(\lambda)_{total} * m\right]$ (19)

where V is the digital voltage measured at wavelength λ, V_O is the extraterrestrial voltage, d is the ratio of the average to the actual earth-sun distance, τ_{total} is the total optical depth, and m is the optical air mass (Holben *et al.,* 1998).

To obtain the aerosol component, optical depth due to water vapor, Rayleigh scattering, and other wavelength-dependent trace gases must be subtracted from the total optical depth equation (20):

$\tau(\lambda)\text{Aerosol} = \tau(\lambda)_{total} - \tau(\lambda)\text{water} - \tau(\lambda)\text{Rayleigh} - \tau(\lambda)O_3 - \tau(\lambda)NO_2 - \tau(\lambda)CO_2 - \tau(\lambda)CH_4$ (20)

The Ängström exponent, (α), provides basic information on the aerosol size distribution. The spectral variations of AOD and α, both are observed corresponding to the aerosol characteristics equation (21) (Holben *et al.,* 2001; Eck *et al.,* 2010).

$\tau_\lambda = \beta\lambda^{-\alpha_A}$ (21)

where τ_λ is aerosol optical thickness or depth at the wavelength (λ in micrometers), while β and α are the Ängström's turbidity coefficient and the Ängström exponent respectively. The Angstrom exponent is often used to give an indication of the relative magnitude of the fine and coarse mode contributions to the total extinction AOD (Eck *et al.,* 2010).

Relationship Between AOD and PM

Some parameters used to describe atmospheric physical conditions change much more in the vertical direction than the horizontal direction. Consequently, it is often assumed that the atmosphere has a structure in which the horizontal direction is uniform and the vertical direction is layered (Xu & Id, 2020). Therefore, for a single homogeneous atmospheric layer containing spherical aerosol particles. The mass concentration at the particular surface is obtained after drying the sampled air, and is represented by equation (22) (Koelemeijer *et al.,* 2006):

$\text{PM} = \frac{4}{3}\pi\rho \int r^3 n(r)dr$ (22)

where ρ denotes the density of aerosol particles (g/m^3) and $n(r)$ describes the aerosol size distribution spectrum under dry conditions. The AOD of the layer with height H is given by equation (23) (Koelemeijer *et al.,* 2006):

$\text{AOD} = \pi \int_0^H \int_0^\infty Q_{ext,amb}(r) n_{amb} r^2 n(r)drdz$ (23)

$\text{AOD} = \pi f(RH) \int_0^H \int_0^\infty Q_{ext,dry}(r) n(r) r^2 n(r)drdz$ (24)

where $n_{amb}(r)$ the size distribution under ambient relative humidity conditions, $Q_{ext,amb}$ is the extinction efficiency under ambient conditions, $Q_{ext,dry}$ the extinction efficiency under dry conditions, and the hygroscopic growth factor f(RH), which represent the ratio between these (size-distribution integrated) extinction efficiencies.

The size-distribution integrated extinction efficiency $\langle Q_{ext} \rangle$ is defined as equation (25) (Koelemeijer *et al.,* 2006).

$\langle Q_{ext} \rangle = \frac{\int r^2 Q_{ext}(r) n(r) dr}{\int r^2 n(r) dr}$ (25)

Effective Radius (r_{eff}) is an area weighted mean radius of the aerosol particles given as equation (26) by (Koelemeijer *et al.,* 2006):

$r_{eff} = \frac{r^3(r) n(r) dr}{\int r^2 n(r) dr}$ (26)

Hence, substituting equations (24), (25), (26) into (23) will produce equation (27) (Koelemeijer *et al.,* 2006; Li, 2015):

$\text{AOD} = \text{PM} \cdot H \cdot f(\text{RH}) \frac{3(Q_{ext,dry})}{4\rho r_{eff}}$ (27)

where H is the height of the aerosols and all the terms retain their usual meanings as above.

Models Performance Indicators

Performance Indicator (PI) measures two things: (1) accuracy measure and (2) error measure. The accuracy measures evaluate values from 0 to 1, whereby the best model is considered when the evaluated values are close to 1, while the best model for error measures will be selected if the evaluated value is close to 0s (Ahmat *et al.,* 2015; Abdullah *et al.,* 2019). Performance indicators for statistical analysis:

i. Correlation Coefficient (R^2):

$R^2 = \left(\frac{\sum_{i=1}^n (P_i - \bar{P})(O_i - \bar{O})}{n.S_{pred} S_{obs}}\right)^2$ (35)

ii. Root Mean Square Error (RMSE):

$RMSE = \left[\left(\frac{1}{n-1}\right) \sum_{i-1}^n (P_i - O_i)^2\right]^{1/2}$ (36)

iii. Mean Bias Error (MBE):

$MBE = \frac{1}{n} \sum_{i=1}^n (P_{est} - P_{obs})$ (37)

iv. Normalized Absolute Error (*NAE*):

$NAE = \frac{\sum_{i=1}^n |P_i - O_i|}{\sum_{i=1}^n O_i}$ (38)

v. Prediction Accuracy (*PA*):

$PA = \sum_{i=1}^n \frac{(P_i - \bar{P})(O_i - \bar{O})}{(n-1) S_{pred} S_{obs}}$ (39)

where n = total number measurements at a particular site, P_{est} = calculated values, P_{obs} = observed values P_i = forecasted values, O_i = observed values, P = mean of forecasted values, O = mean of observed values, S_{pred} = standard deviation of forecasted values and S_{obs} = standard deviation of the observed values.

MATERIALS AND METHODS

The materials used in conducting the research work comprises of; Satellite data obtained from clarity data and purple air devices, Ground data obtained from air quality station, Microsoft excel for sorting, analyzing and comparing data, Internet connection for downloading and accessing websites necessary for the project.

Study Area

Kano is a historic and commercial city in northern Nigeria and serves as the capital of Kano State. It is one of the largest and most economically significant cities in the country, known for its rich cultural heritage, ancient trade routes, and vibrant industries. Located at approximately latitude 12.0022° N and longitude 8.5919° E, Kano has a semi-arid climate with distinct dry and rainy seasons. The city has long been a centre for commerce, agriculture, and Islamic scholarship, playing a vital role in West African trade for centuries.

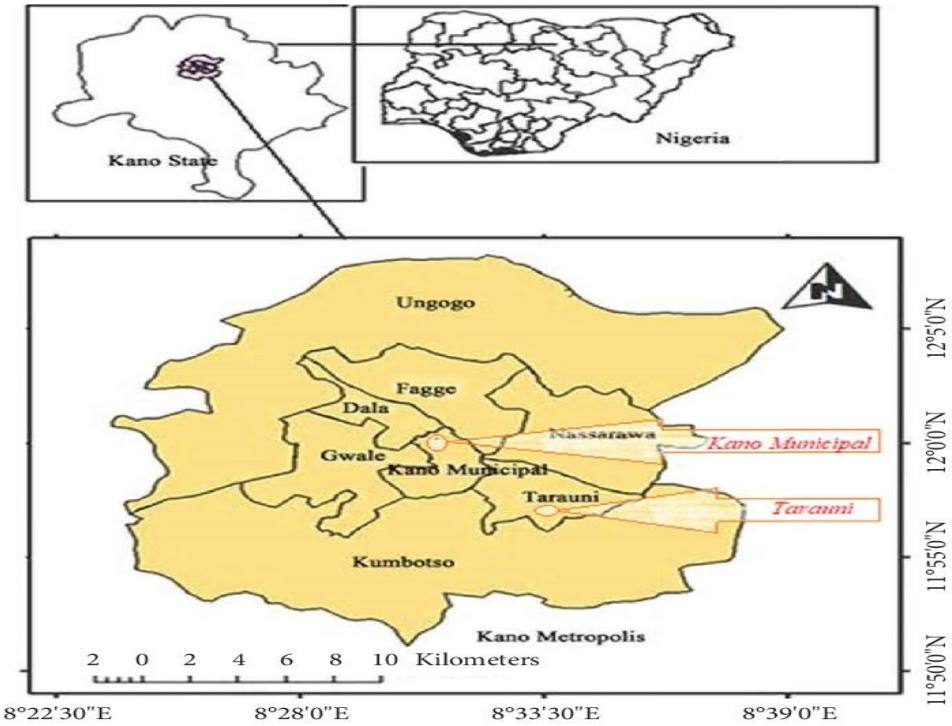

Figure 1: Map of Kano State, Nigeria (Google map, 2025)

Methods

When comparing ground data and satellite data, we need methods that assess their agreement, accuracy, and reliability. Some of the suitable methods are listed below:

Data Collection

$PM_{2.5}$ ground data was obtained from Clarity Data and Purple Air (SWAP lab, department of Physics, BUK) for the period of 12 months and $PM_{2.5}$ Satellite data was obtained from NASA for the period of 12months.

Data Pre-processing

i. Ground Data Processing: Standardizing units, handling missing values, and ensuring consistency.
ii. Satellite Data Processing: Applying radiometric and geometric corrections, resampling, and filtering.

Statistical Analysis

GIS Mapping: Visualizes spatial differences and interpolates missing data

Data Visualization

i. Scatter Plots: Show correlation strength between ground and satellite data.
ii. Time-Series Graphs: Compare trends over time for both datasets.
iii. Histograms & Box Plots: Display data distribution and detect anomalies.

Procedure

This section explains the procedure taken to carry out the analysis which includes data collection, pre-processing, statistical analysis, visualization, and interpretation. The first step is to collect ground-based $PM_{2.5}$ data from Clarity data (μg/m³) and Purple Air which use low-cost sensors to measure air pollution in real time. Satellite-derived $PM_{2.5}$ estimates can be accessed from sources like NASA's Giovanni platform and Google Earth Engine, which provide remote sensing data, including Aerosol Optical Depth (AOD), a parameter often converted into $PM_{2.5}$ using regression models. Purple Air also provides satellite-calibrated $PM_{2.5}$ estimates, which was used directly for comparison.

After collecting the data, pre-processing ensures consistency between the datasets. Since satellite observations capture large-scale air quality trends while ground sensors provide localized measurements, the data must be spatially and temporally aligned. First, the locations of satellite and ground stations must match to ensure meaningful comparisons. Additionally, satellite data was collected at specific overpass times, while ground sensors record continuously, so timestamps must be synchronized (Zhang *et al.,* 2021). It was ensured that both datasets report $PM_{2.5}$ concentrations in micrograms per cubic meter (μg/m³).

When the data was processed, statistical analysis was performed to assess how well the satellite-derived $PM_{2.5}$ estimates match ground-based measurements. A key metric is the Pearson correlation coefficient (r), which measures the strength of the relationship between the two datasets. A value close to 1 indicates a strong correlation, suggesting that satellite data accurately represents $PM_{2.5}$ levels on the ground. Additionally, error metrics such as the Root Mean Square Error (RMSE) and Mean Bias Error (MBE) quantify the level of deviation between satellite and ground values, helping to identify systematic overestimations or underestimations (Zhang *et al.,* 2021). Further, regression analysis was conducted, where a strong agreement was indicated if the slope of the regression line is close to 1 and the intercept is near 0.

To better understand the relationship between ground and satellite data, visualization techniques were used. A scatter plot is commonly employed to display individual comparisons between ground and satellite $PM_{2.5}$ estimates, providing insight into the degree of agreement. Time series analysis allows for the examination of trends over different time periods, highlighting variations in pollution levels. Additionally, geospatial heat maps are useful for visualizing the spatial distribution of $PM_{2.5}$ concentrations, revealing

potential differences between urban and rural areas or areas with varying pollution sources.

The final step is interpretation and conclusion, where the reliability of satellite-derived $PM_{2.5}$ estimates was assessed. If correlation is high ($r > 0.7$) and errors are low, then satellite data can be considered reliable for air quality monitoring in regions with limited ground sensors. However, if discrepancies exist, adjustments may be required, such as incorporating meteorological variables like wind speed, temperature, and humidity to refine the satellite-derived $PM_{2.5}$ estimates (Zhang *et al.,* 2021). This comparative analysis is essential for improving the accuracy of remote sensing data and enhancing air quality monitoring, particularly in regions where ground-based monitoring stations are scarse.

RESULTS AND DISCUSSION

In this research work, the relationship between ground and satellite data of particulate matter ($PM_{2.5}$) in Kano state, Nigeria, covering a period of 12 months from July 2021 to July 2022 was investigated. The study also identified seasonal variations in $PM_{2.5}$ concentrations, with higher levels observed during the Harmattan season.

Table 1a: Monthly comparison of $PM_{2.5}$ ground and satellite data from July to December (2021)

Month (2021)	Purple air (µg/m³)	Clarity data (µg/m³)	Ground data(µg/m³)
July,	21.3954	10.6095	22.3573
August	20.6831	6.5490	13.0860
September	26.0897	10.4376	25.4690
October	26.6978	21.1503	34.3923
November	39.6162	24.1696	35.5245
December	30.1618	15.0793	89.3019

Table 1a, Monthly Comparison of Particulate Matter($PM_{2.5}$) (July to December 2021). The monthly comparison of Particulate Matter ($PM_{2.5}$) concentrations from July 2021 to December 2021 reveals a notable trend (Table 4.1a). The concentrations are relatively low, below 30 µg/m³, from July to October for both ground and satellite data. This is consistent with the rainy season in Nigeria, which typically occurs from May to October (Adejuwon, 2004). According to Adejuwon, (2004) rainfall can reduce aerosol concentrations by washing out particulate matter from the atmosphere. However, in December, the $PM_{2.5}$ concentrations increase, likely due to the onset of the Harmattan season, characterized by dry and windy conditions. As noted by Marticorena *et al.* (2010), the Harmattan season is associated with increased aerosol concentrations due to dust emissions.

Table 1b: Monthly comparison of $PM_{2.5}$ ground and satellite data from January to June (2022)

Month (2022)	Purple air (µg/m³)	Clarity data (µg/m³)	Ground data(µg/m³)
January	28.5132	15.84	82.3693
February	81.6732	18453	78.6971
March	116.7944	26.0463	117.117
April	19.7023	14.2136	50.5872
June	22.5984	15.4248	41.1532

Table 1b shows the monthly comparison of Particulate Matter (2.5) for the period of six months (January 2022 to June 2022). The monthly comparison of $PM_{2.5}$ concentrations from January to June 2022 shows a different trend (Table 5). The concentrations are high from January to March, exceeding 100 µg/m³, consistent with the peak Harmattan period (Ogunjobi *et al.,* 2017). Aerosol concentrations are typically higher during dry seasons due to increased dust emissions. However, in April and June, the PM2.5 concentrations decrease, likely due to the onset of the rainy season, which washes out particulate matter from the atmosphere (Adejuwon, 2004).

Discussion

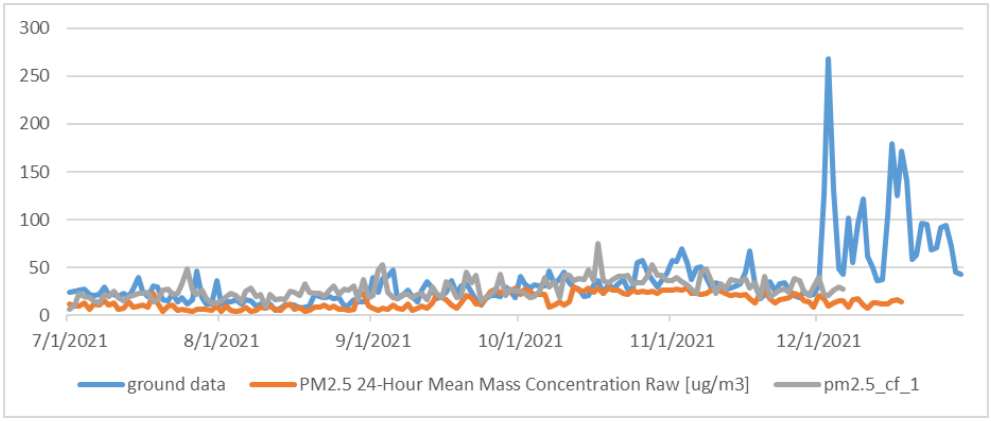

Figure 2a: Compared daily ground data and satellite data from July to December (2021)

The daily ground and satellite data for $PM_{2.5}$ concentrations in Kano, Nigeria, from July to December 2021 shows a notable trend (Figure 2a). The concentrations remain relatively low, below 100 µg/m³, from July to November, consistent with the rainy season in the region (Adejuwon, 2004). However, in December, the concentrations increase, likely due to the onset of the Harmattan season, characterized by dry and windy conditions (Ogunjobi *et al.,* 2017).

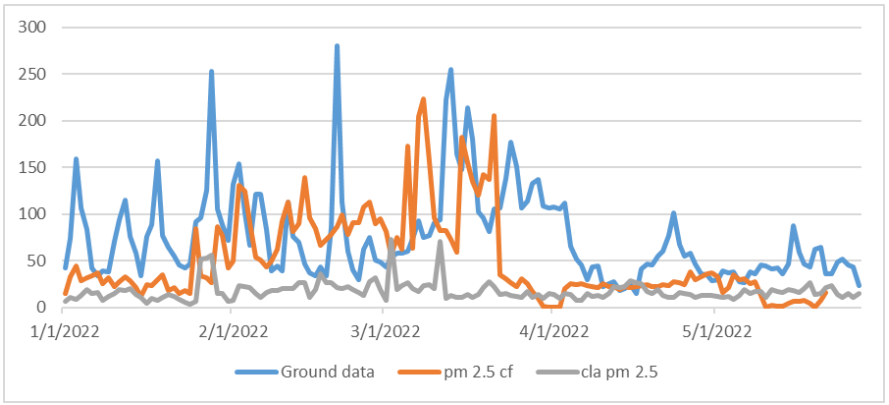

Figure 2b: Compared daily ground data and satellite data from January to June (2022)

The daily data for January to May 2022 reveal high $PM_{2.5}$ concentrations, exceeding 200 µg/m³, particularly during the peak Harmattan period (January-March) (Figure 2b). This is consistent with previous studies, which have reported elevated $PM_{2.5}$ levels during the Harmattan season in West Africa (Marticorena *et al.,* 2010). The concentrations decrease in April and May, coinciding with the onset of the rainy season.

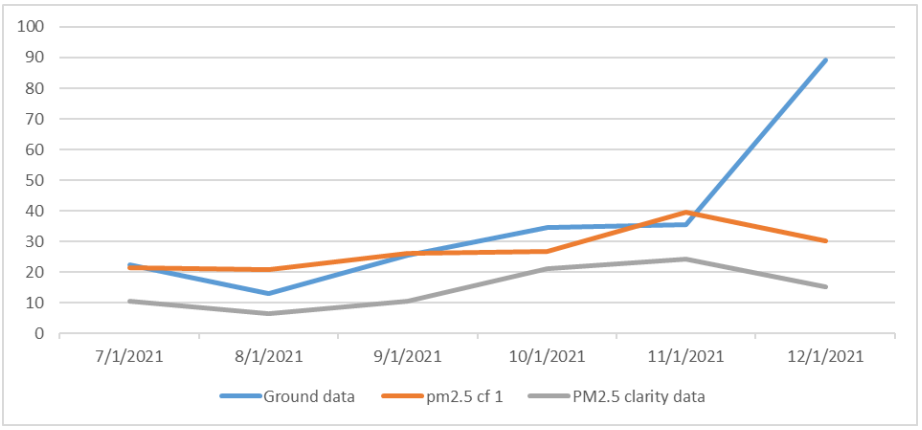

Figure 2c: Compared monthly ground data and satellite data from July to December (2021)

The monthly data for July to December 2021 shows relatively low $PM_{2.5}$ concentrations, below 30 µg/m³, from July to November (Figure 2c). This is attributed to the rainy season, which reduces aerosol concentrations in the atmosphere (Andreae, 2007). However, in December, the concentrations increase to approximately 90 µg/m³, likely due to the Harmattan season.

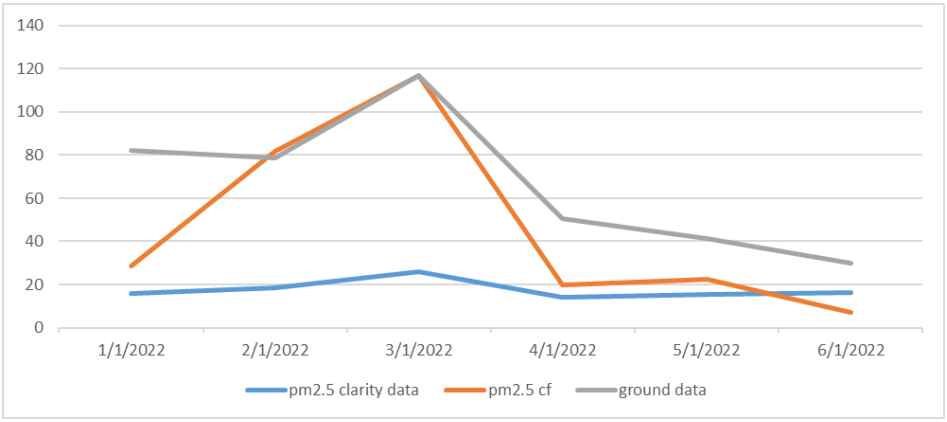

Figure 2d: Compared monthly ground data and satellite data from January to June (2022)

The monthly comparison of particulate matter ($PM_{2.5}$) concentrations from January 2022 to June 2022 reveals a notable trend (Figure 2d). The concentrations are high from January to March, with values exceeding 150 µg/m³, consistent with the Harmattan season in West Africa (Ogunjobi *et al.,* 2017). According to a study published in the Journal of Aerosol Science, the Harmattan season is characterized by high winds and dry conditions, leading to increased aerosol concentrations (Marticorena *et al.,* 2010). As noted by Andreae (2007), aerosol concentrations are typically higher during dry seasons due to increased dust emissions. In contrast, the $PM_{2.5}$ concentrations decrease significantly in April and May, with values below 40 µg/m³, coinciding with the onset of the rainy season. This is consistent with a study published in the Journal of Agricultural and Rural Development, which found that rainfall can reduce aerosol concentrations by washing out particulate matter from the atmosphere (Adejuwon, 2004).

CONCLUSION

The findings of this study demonstrate the potential of satellite data for estimating $PM_{2.5}$ concentrations in Kano state. The results also highlight the importance of monitoring air quality in the region, particularly during the Harmattan season when $PM_{2.5}$ concentrations tend to be higher. Results indicate that during the dry season (Harmattan), $PM_{2.5}$ concentrations reached 270 µg/m³, 117.11µg/m³ and 90µg/m³ highlighting increased pollution due to dust transport and atmospheric stability. In contrast, during the rainy season, $PM_{2.5}$ levels dropped significantly to 6.59µg/m³, 12.5µg/m³, 14.2µg/m³ and 15.42µg/m³ demonstrating the effect of wet deposition. Furthermore, the study findings can be used to raise awareness about the importance of air quality and the need for sustained monitoring and management efforts. Consistent with studies conducted in Minna, Port Harcourt, and Akure, $PM_{2.5}$ levels were observed to be higher during the dry season due to increased atmospheric stability, lower wind speeds, and dust transport from the Sahara Desert (Arowosegbe *et al.,* 2024; Okoro *et al.,* 2019; Olatunde & Adedeji, 2022). Additionally, the Niger Delta study demonstrated that while satellite-derived $PM_{2.5}$ data provide regional insights, local variations such as emissions from biomass burning and industrial activities are better captured by ground-based sensors (Shaibu & Weli, 2017). This aligns with our findings, where satellite data sometimes underestimated peak $PM_{2.5}$ levels recorded by ground sensors, particularly during periods of intense pollution.

REFERENCES

Adejuwon, J. O. (2004). Climate and vegetation in Nigeria. Journal of Agricultural and Rural Development, 2(1), 1-13.

Arowosegbe, A., Adekunle, A., & Ojo, T. (2024). Seasonal variability of $PM_{2.5}$ and meteorological influences in Minna, Nigeria. International Journal of Environmental Sciences, 15(3), 78-92.

Buchhorn, M., Dierckx, S., & Dufour, F. (2020). Sentinel-3 products for air quality monitoring. Copernicus Atmosphere Monitoring Service. https://www.copernicus.eu/en

Cai, S., Lu, X., & Song, Y. (2020). Estimating aerosol optical depth and fine particulate matter (PM 2.5) from satellite data: A review. Science of the Total Environment, 712, 136611. https://doi.org/10.1016/j.scitotenv.2019.136611

Cao, J., Xu, B., & Zhang, L. (2020). Satellite-based monitoring of PM 2.5 using aerosol optical depth. Environmental Pollution, *266*, 115094. https://doi.org/10.1016/j.envpol.2020.115094

Cheng, T., Chen, C., & Xu, L. (2018). Air quality monitoring from satellite: Challenges and applications. Remote Sensing, *10*(12), 2006. https://doi.org/10.3390/rs10122006

Cohen, A. J., Brauer, M., & Burnett, R. (2017). Estimates and 25-year trends of the global burden of disease attributable to ambient air pollution: An analysis of data from the Global Burden of Diseases Study. The Lancet, 389(10082), 1907–1918. https://doi.org/10.1016/S0140-6736(17)30505-6.

Dey, S., & Di Girolamo, L. (2018). Aerosol optical depth retrieval from satellite measurements: Advances and challenges. Remote Sensing, 10(7), 1121. https://doi.org/10.3390/rs10071121

Eck, T. F., Holben, B. N., Sinyuk, A., Pinker, R. T., Goloub, P., Chen, H., … Xia, X. (2010). Climatological aspects of the optical properties of fine/coarse mode aerosol mixtures. *Journal of Geophysical Research Atmospheres*, *115*(19).

Gao, Y., Wang, Z., & Zhang, W. (2015). Monitoring aerosol optical depth and PM 2.5 concentrations from satellite: A case study in China. Environmental Science & Technology, 49(16), 9899–9906. https://doi.org/10.1021/acs.est.5b02444

Google Map (2025). Map of Kano State Nigeria. https://maps.app.goo.gl/W1qwbmrkrm2o9mv96.

Han, Y., Zheng, Y., & Wang, X. (2019). Long-term trends of PM 2.5 concentrations: Satellite-based estimates. Atmospheric Chemistry and Physics, 19(4), 2485–2497. https://doi.org/10.5194/acp-19-2485-2019

He, J., Wang, Y., & Zhang, X. (2020). Recent advances in continuous PM 2.5 monitoring techniques: A review. Science of the Total Environment, 732, 139315. https://doi.org/10.1016/j.scitotenv.2020.139315

Holben, N., Tanr, D., Smirnov, A., Eck, T. F., Slutsker, I., Newcomb, W. W. & Zibordi, G. (2001). An emerging ground-based aerosol climatology: Aerosol optical depth from AERONET. 106(Dll).

Idris, M., Muhammad, G.A., Said, R.S and Akpootu, O.D. (2022) "Effect of Meteorological Parameters on the Dispersion of Vehicular Emission in some Selected Areas in Kano State-Nigeria" Bayero Journal of Pure and Applied Sciences, Volume13, No.1, pp517-524, ISSN: 2006-6996

Idris, M., Darma, T.H., Koki, F.S., Suleiman, A., Ali, M.H., Yarima, S.U. and Aliyu, A. (2020) "An analysis of air Pollution at some Industrial areas of Kano using the AERMOD model" Bayero Journal of Pure and Applied Sciences (BAJOPAS), Special Conference Edition Volume12, No.1, pp117-127, ISSN: 2006-6996, https://doi.org/10.4314/bajopas.v12i1.20S.

Koelemeijer, R. B. A. Ã., Homan, C. D., & Matthijsen, J. (2006). Comparison of spatial and temporal variations of aerosol optical thickness and particulate matter over Europe. 40, 5304–5315. https://doi.org/10.1016/j.atmosenv.2006.04.044

Lawal, H.A., Muhammad, M.I. & Bulus, I. (2023). Atmosphere Hemispheric Analysis of Particulates Pollution over Africa. FUDMA Journal of Sciences 7(4), 272-277. https://doi.org/10.33003/fjs-2023-0704-1924.

Lazrak, N., Zahir, J., & Mousannif, H. (2019). Air Quality Monitoring Using Deterministic and Statistical Methods. https://doi.org/10.1007/978-3-030-12048-1

Li, B., Hou, L., Delta, Y. R., & Area, B. (2015). Discuss On Satellite-Based Particulate Matter Monitoring. Xl(May), 11–15. https://doi.org/10.5194/isprsarchives-XL-7-W3-219-2015

Liu, Y., Xia, Y., & Yin, X. (2019). Exposure to PM 2.5 and human health: A review of the global and regional health risks. Environmental Pollution, *254*, 113037. https://doi.org/10.1016/j.envpol.2019.113037

Liu, Y., Sarnat, J. A., Coull, B. A., Koutrakis, P., & Jacob, D. J. (2004). Validation of Multiangle Imaging Spectroradiometer (MISR) aerosol optical thickness measurements using Aerosol Robotic Network (AERONET) observations over the contiguous United States. Journal of Geophysical Research: Atmospheres, 109(6), 1–9. https://doi.org/10.1029/2003jd003981

Muhammad, M. Said, R.S, Tijjani B.I., Idris, M., Sani, M. (2022). Investigating the effect of altitude and meteorological parameters on the concentration of particulate matter at an urban area of Kano state, Nigeria. Bayero journal of pure and applied sciences, 13(1): 400 – 408, ISSN 2006 – 6996. http://dx.doi.org/10.4314/bajopas.v13i1.61s.

Musa, A. (2010). Principles of Photovoltaic Energy Conversion. Ahmadu Bello University Press Limited, Zaria.

Ostro, B. D., Broadwin, R., & Green, S. (2019). Fine particulate air pollution and mortality in 20 US cities: A report from the American Cancer Society. Environmental Health Perspectives, *127*(10), 107009. https://doi.org/10.1289/EHP4747

Okoro, C. A., Nwankwo, E. O., & Eke, P. C. (2019). Assessment of $PM_{2.5}$ and PM_{10} concentrations in Port Harcourt: Meteorological influences. Journal of Atmospheric Pollution Research*, 10(2), 157-169.*

Olatunde, J. A., & Adedeji, A. (2022). Effects of seasonal variation on air quality: A case study of Akure, Southwestern Nigeria. Atmospheric Science Journal*,* 14(7), 543-558.

Ouedraogo, S., Kouadio, A., & Mensah, A. (2024). Long-term variability of $PM_{2.5}$ concentrations in Abidjan and Accra: The role of Harmattan dust transport. Environmental Advances, 12, 104-118.

Shaibu, S., & Weli, V. (2017). Satellite-based assessment of $PM_{2.5}$ distribution in the Niger Delta region. International Journal of Research in Environmental Science*,* 3(2), 1-12.

Xu, X., & Id, C. Z. (2020). Concentration using MODIS AOD and corrected regression model over Beijing, 1–15. https://doi.org/10.1371/journal.pone.0240430

Zhang, L., Nin, Y., Ghau, F. (2021). Validation of satellite-derived $PM_{2.5}$ estimates over different regions. Atmospheric Research, 248, 105213.